Int. J. Heat Mass Transfer. Vol. 17, pp. 567–579. Pergamon Press 1974. Printed in Great Britain

MASS TRANSFER FROM AERODYNAMICALLY ROUGH SURFACES

S. B. VERMA* and J. E. CERMAK
Fluid Dynamics and Diffusion Laboratory, College of Engineering,
Colorado State University, Fort Collins, Colorado 80521, U.S.A.

(*Received* 30 *March* 1973 *and in revised form* 27 *September* 1973)

Abstract—Mass transfer rates were determined by directly measuring the actual volume of water evaporated from saturated wavy (sinusoidal) surfaces in a micrometeorological wind tunnel. Simultaneous measurements of mean velocity, humidity and temperature distributions were made over these saturated waves. Under equilibrium boundary layer conditions, the average mass transfer coefficient was found to be a simple power function of the surface Reynolds number, $u_* z_0/\nu$. Based on this result the mass transfer data from this study correlated well with published mass transfer data from various other types of surfaces, e.g. water waves, flat plate, and surfaces roughened with pyramids and spanwise humps.

NOMENCLATURE

a, wave amplitude [L];

C_f, effective average skin friction coefficient

$$= \frac{\tau_0}{\frac{1}{2}\rho U_\infty^2} \text{ [dimensionless]};$$

C_p, specific heat at constant pressure $[HM^{-1}\theta^{-1}]$;

d, zero plane displacement [L];

D, molecular mass diffusivity $[L^2T^{-1}]$;

E, evaporation rate per unit area $[ML^{-2}T^{-1}]$;

g, acceleration due to gravity $[LT^{-2}]$;

H, form factor [dimensionless];

H_0, heat flux $[HL^{-2}T^{-1}]$;

h, wave height [L];

k, Karman constant [dimensionless];

K_z, exchange coefficients of water vapor in z direction $[L^2T^{-1}]$;

L, Monin–Obukhov length [L];

l, characteristic length [L];

m, n, exponents [dimensionless];

p_∞, free stream static pressure $[ML^{-1}T^{-2}]$;

Pr, Prandtl number [dimensionless];

q, specific humidity

$$\left(\frac{\text{g of water vapor}}{\text{g of dry air}}\right) \text{ [dimensionless]};$$

q_{amb}, ambient specific humidity

$$\left(\frac{\text{g of water vapor}}{\text{g of dry air}}\right) \text{ [dimensionless]};$$

q_s, surface air humidity

$$\left(\frac{\text{g of water vapor}}{\text{g of dry air}}\right) \text{ [dimensionless]};$$

q_∞, specific humidity in free stream

$$\left(\frac{\text{g of water vapor}}{\text{g of dry air}}\right) \text{ [dimensionless]};$$

Δq, difference of the surface and ambient concentrations [dimensionless];

Re, Reynolds number [dimensionless];

$(Re_*)_0$, surface Reynolds number

$$= \frac{u_* z_0}{\nu} \text{ [dimensionless]};$$

Sc, Schmidt number $= \frac{\nu}{D}$ [dimensionless];

Sh, Sherwood number [dimensionless];

$(Sh)_h$, Sherwood number based on h [dimensionless];

$(Sh)_l$, Sherwood number based on l [dimensionless];

$(Sh)_0$, Sherwood number based on z_0 [dimensionless];

T, temperature $[\theta]$;

U, mean velocity components in X direction $[LT^{-1}]$;

U_∞, free stream mean velocity in x direction $[LT^{-1}]$;

u_*, friction velocity $[LT^{-1}]$;

x, distance along longitudinal direction [L];

y, distance along lateral direction [L];

z, distance above effective zero plane in vertical direction [L];

*Now at University of Nebraska, Lincoln, Nebraska 68503, U.S.A.

z_c, distance above wave crest in vertical direction [L];
z_T, distance above wave bottom in vertical direction [L];
z_0, roughness parameter [L];
ν, coefficient of kinematic viscosity [L^2T^{-1}];
ρ, mean mass density [ML^{-3}];
τ_0, effective wall shear stress [$ML^{-1}T^{-2}$];
λ, wave length [L];
δ, boundary layer thickness [L];
δ^*, displacement thickness [L];
θ, momentum thickness [L].

INTRODUCTION

IN A SO-CALLED "aerodynamically smooth flow", the drag exerted on the fluid by the boundary surface is a function of the Reynolds number only, and, except for a region very close to the surface, the distribution of mean velocity is represented by

$$\frac{U}{u_*} = \frac{1}{k} \ln \frac{u_* z}{\nu} + 5{\cdot}5. \tag{1}$$

On the other hand, for "aerodynamically rough flows", the drag is independent of the Reynolds number and is proportional to the square of velocity with the mean velocity distribution given by

$$\frac{U}{u_*} = \frac{1}{k} \ln \frac{z}{z_0} \quad \text{for} \quad z > z_0 \tag{2}$$

in which z_0 is the roughness parameter and z is measured from effective zero plane, given by $z = z_T - d$, where z_T is the height measured from the base of the roughness, and d is the zero plane displacement.

Considerable amount of work has been done on mass transfer from aerodynamically smooth surfaces in turbulent flows, but, on the other hand, relatively little has been published on the effect of roughness on the rates of mass (or heat) transfer. Moreover, the results from different investigations (e.g. Nunner [1], Smith and Epstein [2], Dipprey and Sabersky [3], Pohl [4], Kolar [5, 6], etc.) sometimes disagree either partly or completely. Kolar [5, 6] presented a theoretical analysis of heat (or mass) transfer in the turbulent flow of fluids through smooth and rough tubes. His analysis was based on description of the hydrodynamic relations derived from the statistical theory of turbulence. Levich [7] proposed that if the height of roughness was greater than the thickness of the viscous sublayer but less than the turbulent boundary layer, the hydrodynamic situation may be modified in such a way that a decrease in the mean mass transfer would result. He proposed a theoretical correlation for mass transfer rate in terms of friction velocity, difference of surface and free stream concentrations, fluid properties and height of roughness. Although Levich's model presents a basic approach to the problem of mass transfer from rough surfaces, its applicability is limited to $Sc \gg 1$. In a recently published work, Dawson *et al.* [8] reported measurements of mass transfer coefficients for a series of geometrically similar rough surfaces (V-shaped grooves of 2·14 mils depth normal to the flow direction), using an electrochemical technique. For $390 < Sc < 4600$ and Reynolds numbers greater than 15000, their data correlated as

$$\frac{(St)_R}{(St)_S} = f\left(\frac{eu_*}{\nu}, Sc\right)$$

where $St = Sh/ReSc$ is the Stanton number, e is the roughness height and subscripts R and S refer to rough and smooth surfaces respectively.

A few analytical approaches by some meteorologists, e.g. Sutton [9], Calder [10], Rider *et al.* [11] attempted to predict mass transfer rates by solving the diffusion equation. These solutions, however, fail to consider the effect of change in aerodynamic roughness on momentum transfer. A number of field investigations have tried to understand the mechanism of mass transfer from the Earth's surface, but the resulting measurements are difficult to interpret.

The foregoing discussion reveals that the information on mass transfer from rough surfaces is very limited. In view of this, and because of the difficulty of controlling the variables encountered in field research and because of the great amount of time and money involved, laboratory investigation of this problem was initiated at the Fluid Dynamics and Diffusion Laboratory of Colorado State University. The work reported here is part of a comprehensive research program designed to study the transfer of both mass and momentum from rough surfaces. Wavy surfaces were chosen to represent a controlled and defined shape of roughness.

EQUIPMENT AND MEASURING PROCEDURES

Experiments were conducted in a low speed wind tunnel. This recirculating tunnel can generate wind speeds ranging from 5 ft per s to about 70 ft per s. The test section is about 30 ft long and has approximately a 6 ft by 6 ft cross section. The measurements were taken on sinusoidal waves of three different sizes ($\lambda = 4{\cdot}2$ in. and $h = 1{\cdot}70$ in., 1·0 in. and 0·50 in.). These waves were cut from styrofoam blocks with a single shaper blade on a horizontal milling machine. Figure 1 shows the layout of the experimental arrangement in the wind tunnel. The styrofoam waves were laid in

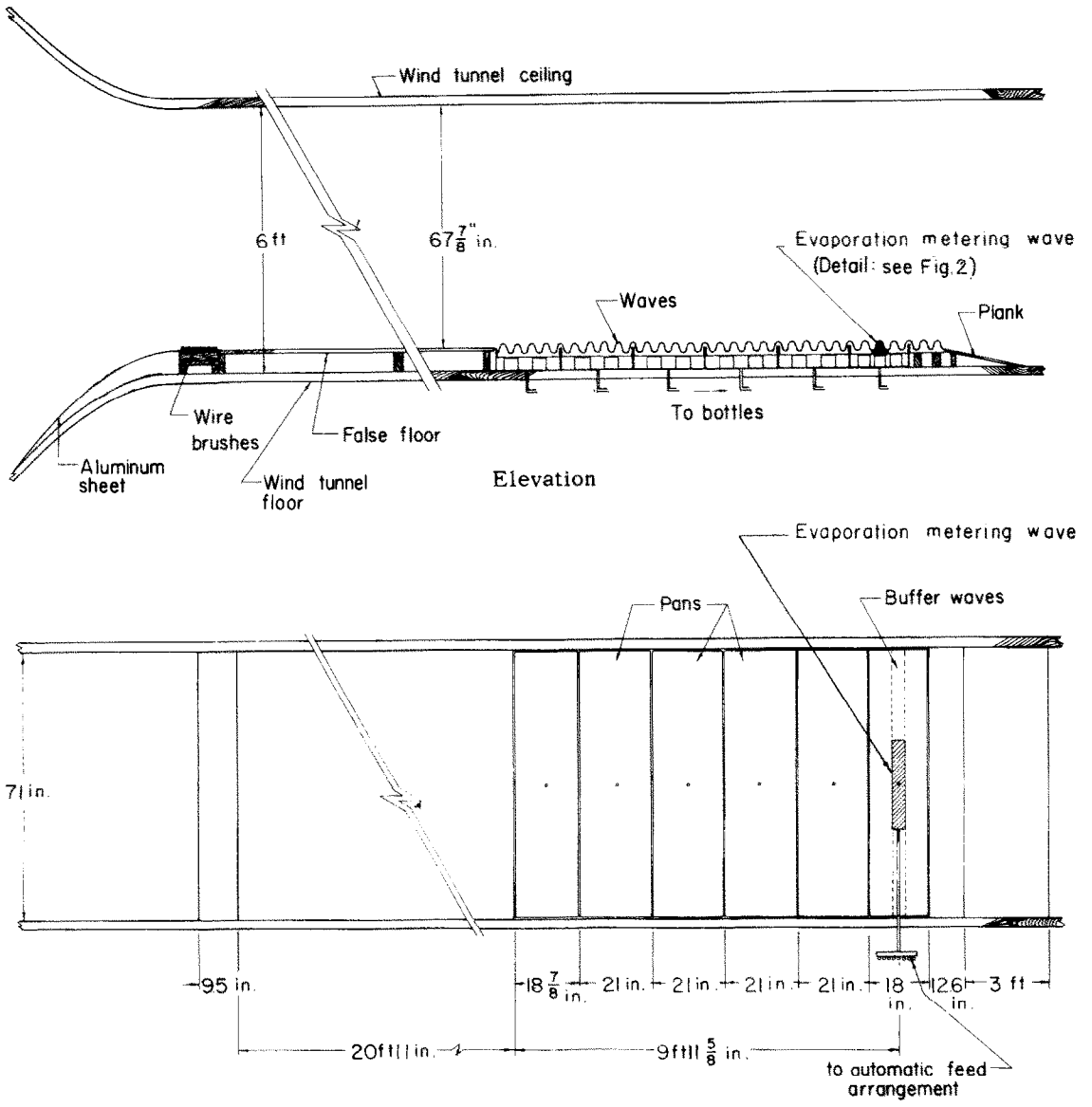

FIG. 1. Experimental arrangement (wave assembly) in wind tunnel.

aluminium pans, which were connected to water reservoirs (Fig. 2) and arrangement was made so that the water level in the pans was maintained up to the wave troughs. A sheet of felt was positioned carefully over the waves, following their contour. When positioning the individual styrofoam waves in the pans, care was taken to leave a small (about 1/32 in. wide) crack between each wave to allow water to flow up from the bottom of the pans (Fig. 2); thus, the continuity of the wavy surface was not disturbed. Before beginning an experimental run, the felt on the styrofoam waves was saturated with water and it was observed that it remained wet everywhere as long as the desired water level in the pans was maintained. Downstream of the 26th styrofoam wave (Fig. 1) a specially built wave (of same size) called "evaporation metering wave", was

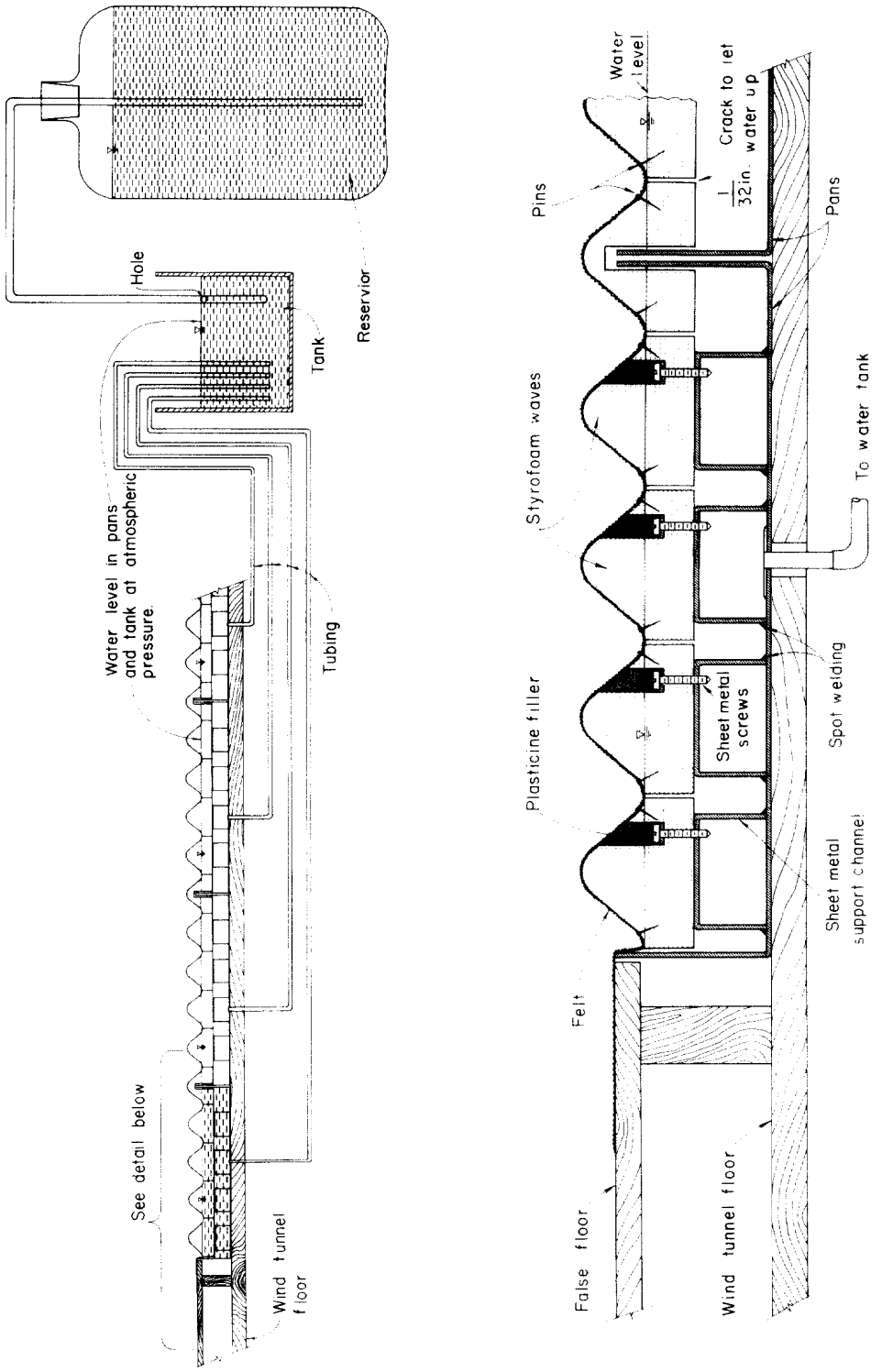

FIG. 2. Details of Fig. 1 (schematic).

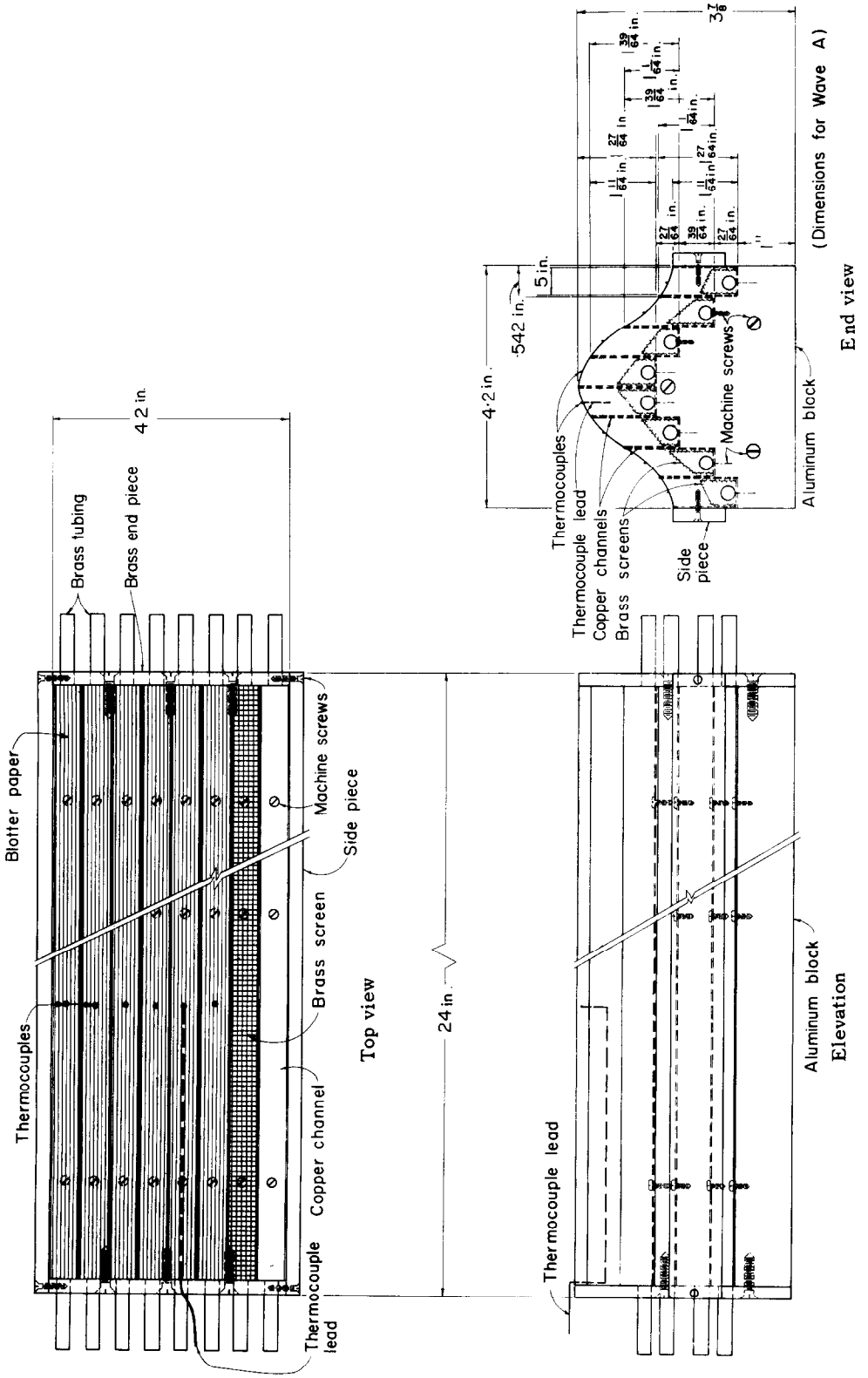

FIG. 3. Evaporation metering wave.

placed in the pans with other styrofoam waves following it. The "evaporation metering wave" (Fig. 3), with the aid of an "automatic feed and metering system" (Fig. 4), facilitated the determination of evaporation rates by measuring the actual volume of water that had evaporated in a given time. This metering wave was divided into eight sections of equal width with thin copper baffles. Strips of blotter paper were cut to fit vertically in these sections; the tops of the blotter papers were carefully sanded to form a continuous surface. Water from separate burettes, belonging to the "automatic feed and metering system", was supplied to the bottom of each section of the metering wave. It was carried to the top of the blotters by capillary action.

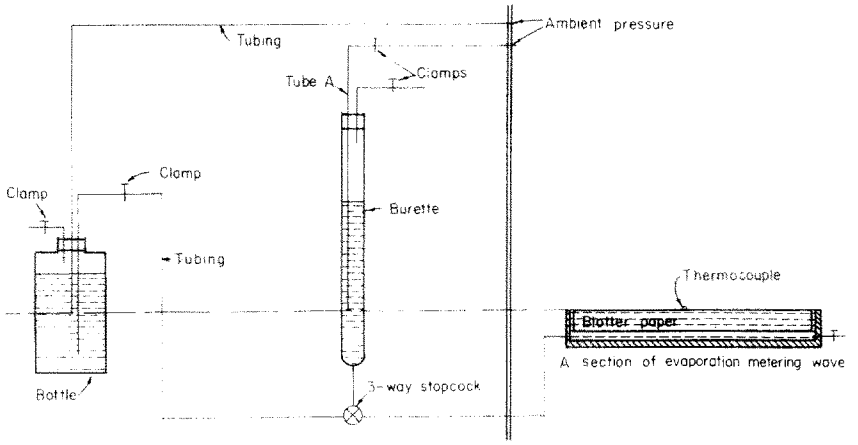

FIG. 4. Part of automatic feed and metering system (typical for each wave section).

The blotter surface was kept wet as long as the water supply was maintained. The pressure difference, created by the water loss from evaporation at the top of each wave section, was compensated for by drawing water from the corresponding burette automatically. The amount of water that evaporated from each section in a given time was measured from the drop of water level in the corresponding burette. The "evaporation metering wave" and the "automatic feed and metering system" were actually designed to measure the distribution of local evaporation rates over the wavy surfaces intended for other related studies and have been described in detail elsewhere [12]. For this study, the average evaporation rates were obtained by integrating the measured local evaporation losses.

The moisture content of the air flow was measured by sampling the gas stream through a stainless steel sampling probe, connected to a dew-point hygrometer (Cambridge Systems, Model 992) at a constant flow rate maintained by a vacuum pump built in the hygrometer. During an experimental run, the background humidity changed with time, although very slowly, because the recirculating air gradually absorbed additional moisture. Also, the surface air humidity changed slightly. Two sampling probes were used simultaneously to measure both the local moisture content in the boundary layer and the free stream moisture content. In addition, the surface air humidity was determined by measuring the surface air temperature T_s by copper constantan thermocouples (mounted on the wave surface), after assuming that it was equal to the saturated humidity at temperature T_s.

In addition to the humidity distribution, the mean velocity and mean temperature fields were also mapped at several longitudinal positions over the wavy surface. The mean velocity distributions were measured by a pitot tube. A set of two hot wires were employed to crosscheck the values obtained by the pitot tube measurements. The mean temperature distributions were measured by copper–constantan thermocouples.

The pressure distribution on the surface of the waves was measured by a special pressure tapped wave, placed at 27th wave position. This pressure tapped wave had the same shape and dimensions as the other styrofoam waves, except that 17 equispaced pressure holes were drilled across the mid section of the wave.

The drag force on the waves was determined by integrating the wall pressure distribution. The results of the drag force measurements were crosschecked by using a shear plate, designed by Hsi and Nath [13].

RESULTS AND DISCUSSION

Velocity fields

A typical set of mean velocity profiles (U/U_∞ vs. z_c/δ) at different crest positions is plotted in Fig. 5, in which z_c is the height measured above the respective wave crests and δ is the boundary layer thickness. Figure 5 clearly shows the changes in the velocity profiles proceeding downstream. However, for stations downstream of the 22nd crest, all the nondimensional velocity profiles approximately collapse into a single curve. In addition, the quantities u_*/U_∞ and dp_∞/dx became almost constant for $x \geqslant 7$ ft (i.e. downstream of the 22nd crest), where x is measured from the start of the leading wave [12]. This means that the boundary layer reached its equilibrium condition in the far downstream region, $x \geqslant 7$ ft [12 and 14]. Typical plots of relevant boundary layer parameters, e.g. boundary layer thickness δ, displacement thickness δ^*, momentum thickness θ, and form factor H are shown in Fig. 6. When the smooth wall boundary layer encounters a series of waves, the form drag of the waves introduces an increase in the wall shear stress. This increase in wall shear stress causes a loss in momentum and therefore, δ, δ^* and θ are increased at a faster rate in the beginning. Shortly however, the flow adjusts itself to a normal boundary layer development, and equilibrium boundary layer conditions are obtained.

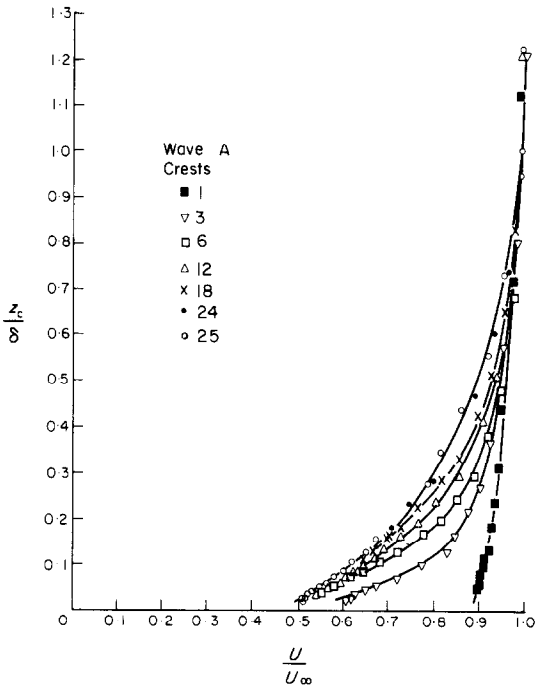

FIG. 5. Mean velocity profiles (typical).

Friction velocities were obtained primarily from the measurements of mean velocity profiles. The results from drag force measurements were used to cross check these values. In order to obtain u_* and z_0, it was assumed that the velocity distribution followed the logarithmic profile

$$\frac{U}{u_*} = \frac{1}{k} \ln \frac{z}{z_0} \quad z > z_0 \tag{2}$$

for nearly neutral conditions. In equation (2), $z = z_T - d = z_c + \varepsilon$ and $\varepsilon = h - d$, where z_T is the height measured from the bottom of the waves, z_c is the height measured above the respective wave crests, d is the zero plane displacement, and h the wave height. The value of d

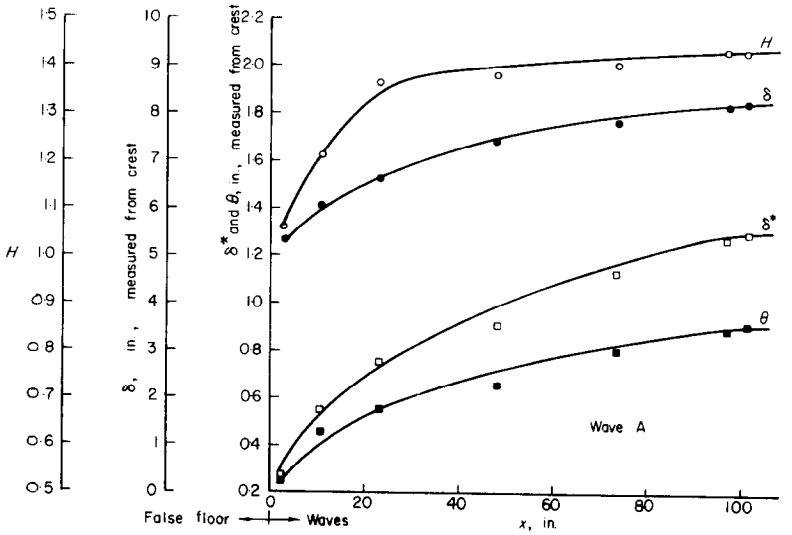

FIG. 6. Plots of δ, δ^*, θ and H (typical).

was estimated by a method similar to the one used by Perry *et al.* [15]. The velocity profiles on wave crests in the far downstream region were first plotted on the U/U_* vs. z_* axes. An estimate of the required slope of the final logarithmic distribution $= (1/k)\ln\sqrt{C_f/2}$, where C_f is the effective average skin friction coefficient $= 2(u_*/U_*)^2$, was calculated using the results from drag measurements [12]. Values of ε were then added to the abscissa of the raw profile in a trial and error process until a value of ε, which gave a straight line with a slope close (within 10 per cent) to the above predetermined value of $(1/k)\ln\sqrt{C_f/2}$, was obtained. The values of $d(=h-\varepsilon)$ so obtained were given by $d/h = 0{\cdot}5, 0{\cdot}25$ and 0 approximately for waves A, B, and C, respectively, with $h/\lambda = 0{\cdot}41$, $0{\cdot}24$ and $0{\cdot}12$. This means from the bottom of the waves, the effective zero plane is raised by about a half and a quarter of the wave height for the steepest and the intermediate waves, but remains unchanged for the shallowest one, which seems reasonable.

Considering the above and using the equation (2), values of z_0 were computed. In the far downstream region, the values of z_0 varied from 0·03 to 0·175 in. for the three wave sets, which are comparable, at least with regard to the order of magnitude, to the results obtained in investigations above similar surfaces [e.g. Chamberlain [16] and Owen and Thomson [17]].

In the evaporation experiments, a temperature gradient was set up as heat was transferred from the air to the evaporating surface. However, the gradient of windspeed in the lowest few inches (above the wave crests) was large, and a typical value of the Richardson number

$$= \frac{g}{T}\frac{\partial T}{\partial z}\left(\frac{\partial U}{\partial z}\right)^{-2},$$

for 1 in. $< z_* <$ 4 in., was found of the order of 10^{-3} (the Monin–Obuklov parameter

$$L = -\frac{u_*^3}{k\dfrac{g}{T}\left(\dfrac{H_0}{\rho C_p}\right)}$$

was of the order of 10^3 cm). Considering the Monin–Obukhov log-linear law

$$\left[\frac{U}{u_*} = (1/k)\left[\ln\frac{z}{z_0} + \beta\frac{z-z_0}{L}, \text{ with } \beta \approx 5\right]\right],$$

an error of about 2 per cent may be involved in estimating u_* by using equation (2).

Average evaporation rates

Average evaporation rates, in the fully developed (far downstream) region, were obtained by direct measurements (described in the previous section). These results were cross checked with another method of computing evaporation rates. This method, which may be called a mass balance method, makes possible the evaluation of evaporation rates by using the equation

$$E = \frac{\mathrm{d}}{\mathrm{d}x}\int_0^{z'} \rho U(z)[q(z) - q_r]\,\mathrm{d}z. \qquad (3)$$

This equation can be obtained by considering a mass balance on a control volume in the air [18].

In the far downstream region, the results obtained from the mass balance method agreed, within 10 per cent, with the direct measurements. Considering that the mass balance method used an entirely different set of measurements than those used for direct evaporation measurements, the agreement is encouraging.

Using the mean velocity and humidity profile measurements made at several longitudinal positions over these waves, the variation of evaporation rates with fetch was obtained as shown in Fig. 7 (typical).

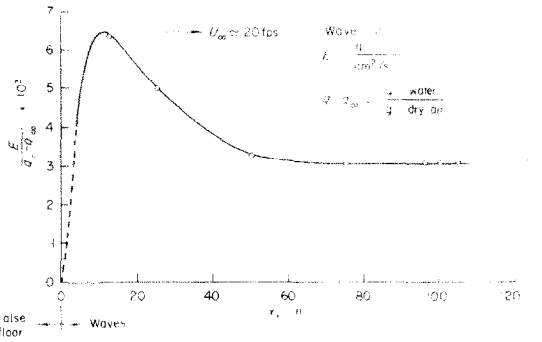

FIG. 7. Variation of average evaporation rates with fetch (typical).

The evaporation rate, in the beginning, increases rapidly to a maximum near the fourth or fifth crest and then decreases, levelling off in the far downstream region. When the relatively dry air contacts the first few waves, it absorbs considerably more moisture than it does in the downstream region. The evaporation rate later decreases and becomes constant in the far downstream region. This kind of variation is compatible with results reported in some other studies, e.g. Marciano and Harbeck [19].

Correlation of evaporation data

For a fully developed boundary layer under nearly neutral conditions, with no lateral diffusion present, a dimensional analysis of the problem of evaporation from a uniformly saturated surface leads to

$$(Sh)_l = \frac{El}{\rho D(q_s - q_r)} = f\left[\frac{u_* l}{\nu}, \frac{\nu}{D}\right] \qquad (4)$$

in which E is the evaporation rate per unit of projected area, ρ is the density, D is the molecular diffusivity, ν is the kinematic viscosity, u_* the friction velocity, $(q_s - q_\infty)$ is the difference of the surface and ambient air humidities, and l is a characteristic length. In this study, an approximately fully developed boundary layer was obtained near the evaporation metering wave. The effect of lateral diffusion was minimized by keeping the buffer waves, located at both ends of the metering wave, completely wet during the course of an experimental run. It has been shown that the conditions in this study could be treated as nearly neutral with a negligible effect of stability on u_*. Therefore, the evaporation data of this study could be correlated on the basis of equation (4).

To start with, wave height h was used as a characteristic length for correlating the data. Values of

$$(Sh)_h = \frac{Eh}{\rho D(q_s - q_\infty)} \quad \text{and} \quad (Re_*)_h = \frac{u_* h}{\nu},$$

for all three wave sets at different free stream speeds, were computed and plotted on Fig. 8. The data is approximately correlated by

$$(Sh)_h = 0{\cdot}10\,(Re_*)_h^{0{\cdot}84}. \tag{5}$$

In connection with mass (or heat) transfer relations of above type, various values have been proposed for the exponent to the Reynolds number. Based on their heat transfer measurements for flow through rough tubes, Kolar [6] and Nunner [1] found values of 0·986 and 1·0 respectively, for the exponent to the Reynolds number formed from the friction velocity and diameter of the tube. On the other hand, Levich [7] obtained

$$\frac{Eh}{\rho D(q_s - q_\infty)} = \left(\frac{u_* h}{\nu}\right)^{1/2} (Sc)^{1/4} \tag{6}$$

where h is the height of protrusions. It should be noted that Levich's analysis is restricted only to cases where $Sc \gg 1$; his results are in good agreement with Mahato and Shemilt's [20] observations (with $Sc = 258$). However, based on his evaporation data from water waves ($Sc = 0{\cdot}6$), Lai [21] reports a $Re^{0{\cdot}85}$ dependence of the Sherwood number.

The applicability of equation (5) is limited to wavy surfaces. In an attempt to make the correlation more general, the roughness parameter z_0 was used as the characteristic length and the results are shown in Fig. 9. The relation

$$(Sh)_0 = 0{\cdot}055\,(Re_*)_0^{0{\cdot}90}, \tag{7}$$

$$\text{with } (Sh)_0 = \frac{Ez_0}{\rho D(q_s - q_\infty)} \text{ and } (Re_*)_0 = \frac{u_* z_0}{\nu},$$

gives the best fit correlation for all the different sets of data. This correlation is applicable to mass transfer from various types of surfaces, some examples of which are considered next.

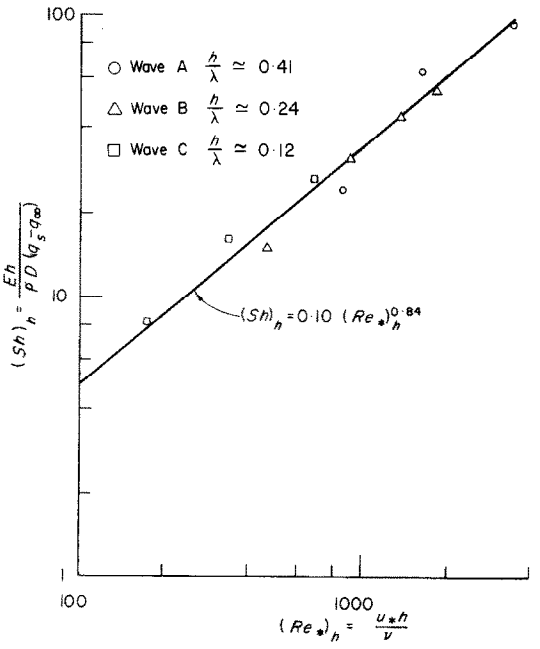

FIG. 8. Correlation of evaporation data with h as the characteristic length.

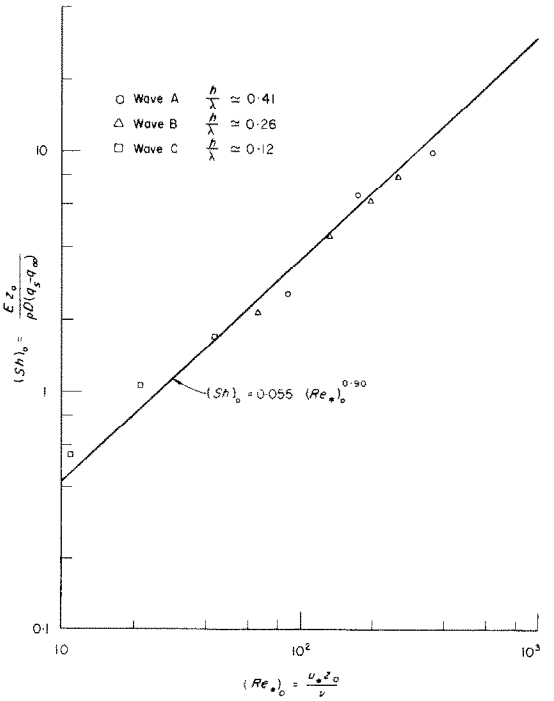

FIG. 9. Correlation of evaporation data with z_0 as the characteristic length.

Comparison with evaporation data from water waves

Lai [21] measured evaporation from small amplitude wind generated water waves at different ambient conditions. He reported his evaporation data along with the corresponding values of the friction velocity u_* and the roughness parameter z_0 obtained from the relation

$$\frac{U}{u_*} = \frac{1}{k} \ln \frac{z}{z_0}, \tag{8}$$

where U is the air speed, k is the Karman constant, and z is the height above mean level. In attempting to correlate Lai's data with the data obtained in the present study, the following considerations can be made. Consider the simplified case of a long train of waves with amplitude a and length λ moving at a constant speed c. The wind blows over these waves with a velocity U which varies with height z, i.e. $U = U(z)$, but remains constant with time and direction. The flow is unsteady and the boundary conditions are different from those of a fixed set of solid waves. To reduce this situation to a steady one, a coordinate system moving at the same speed as the waves is introduced. When viewed from the moving coordinate system, the wave profile is stationary; so this transformation makes boundary conditions correspond approximately to the rigid waves. The introduction of this moving coordinate system does not affect the values of u_* reported by Lai [21], but it does modify the roughness parameter:

$$\frac{(z_0) \text{ moving coordinate}}{(z_0) \text{ fixed coordinate}} = e^{kc/u_*}. \tag{9}$$

Using this modification, values of

$$(Sh)_0 = \frac{Ez_0}{\rho D(q_s - q_z)} \quad \text{and} \quad (Re_*)_0 = \frac{u_* z_0}{\nu}$$

were computed from the set of data, (taken in the approximately fully developed region), reported by Lai. The results are shown in Fig. 10; the evaporation data from the water waves and those from the fixed waves are reasonably well correlated by equation (7).

Comparison with evaporation data from a flat plate

Cermak and Lin [22] reported evaporation results from their experiments on a smooth flat plate. To correlate their data with that of the present study, one needs the values of the friction velocity u_* and the roughness parameter z_0 corresponding to each evaporation run. The values of u_* reported by the authors were based on the relation

$$\frac{U}{u_*} = \frac{1}{k} \ln \frac{zu_*}{\nu} + \text{constant}. \tag{10}$$

For a smooth flat plate, designating z_0 as the roughness parameter may be misleading. However, for the sake of

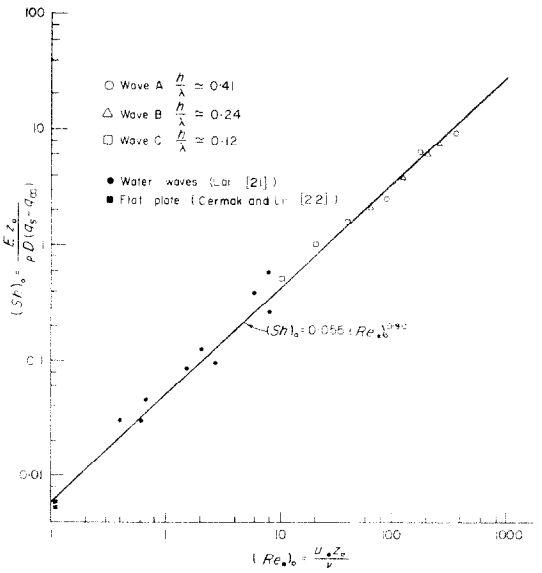

FIG. 10. Correlation of water waves and flat plate data with the data of this study.

evaluating equation (7), z_0 may be assumed to have that value of z for which the extrapolated value of U is zero. This procedure for obtaining z_0 for a flat plate has been previously used by Cermak and Koloseus [23] and Chamberlain [16]. Using the values of u_* and z_0 thus obtained, along with the evaporation data obtained from a flat plate located in a fully developed boundary layer [22], the values of Sherwood number $= Ez_0/\rho D(q_s - q_z)$ and surface Reynolds number $= u_* z_0/\nu$ were computed; the results are shown in Fig. 10. The line representing equation (7), which correlated the data from the solid and water waves, can be extrapolated to correlate the evaporation data from a flat plate reasonably well.

Comparison with sublimation data from different rough surfaces

Owen and Thomson ([17], p. 327) measured sublimation rates of camphor from surfaces roughened by two types of glass: "one was mottled by irregular pyramids in relief and the other reeded, with the generators of the reed running perpendicular to the stream...". To correlate their sublimation data with the evaporation data, one must account for the difference in molecular diffusivities of the camphor and water vapors which can be incorporated in the non dimensional Schmidt number, $Sc = \nu/D$ analogous to the Prandtl number in the corresponding heat transfer case. Thus a correlation of the type,

$$(Sh)_0 \approx (Re_*)_0^m (Sc)^n \tag{11}$$

can be attempted, in which $(Sh)_0 = Ez_0/\rho D(\Delta q)$ where E is the mass transfer rate per unit area and Δq is the difference of the surface and ambient concentrations. A variety of values, ranging from 0·25 to 0·5, for the exponent n have been used in the literature. From their experiments on evaporation of various liquids, Smolsky and Sergeyev [24] reported a value of 0·44 for n as did Gilliland and Sherwood [25]. Levich [7], and Mahato and Shemilt [20] used $Sc^{0.25}$ in their correlation. In heat transfer experiments, Chilton and Colburn [26], Reynolds *et al.* [27], and many others report a $Pr^{0.33}$ dependence, whereas Kolar [6] obtained a $Pr^{0.5}$ dependence on the Nusselt number. In this study, $n = 0.33$ has been chosen for correlating the sublimation data with the evaporation data. Figure 11 shows a plot of $(Sc)_0/(Sc)^{0.33}$ vs $(Re_*)_0$ for the sublimation data of Owen and Thomson [17] with the evaporation data of this study. The line

$$\frac{(Sh)_0}{(Sc)^{0.33}} = 0.064\,(Re_*)_0^{0.90} \tag{12}$$

correlates both of these data well.

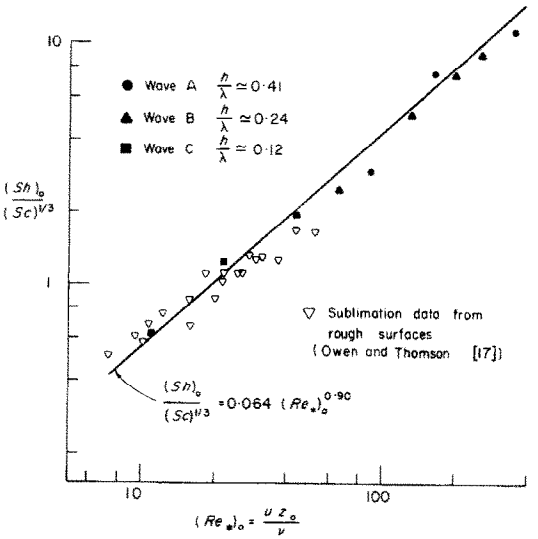

FIG. 11. Correlation of sublimation data from different kinds of rough surfaces (Owen and Thomson [17]) with the evaporation data of this study.

It is important to note that the data points used in the evaluation of equation (12) are limited to small Schmidt numbers, e.g. $Sc \approx 0.62$ (this study) and $Sc \approx 3.2$ (Owen and Thomson). Therefore, care should be taken in using this equation for a wide range of Schmidt numbers.

Comparison with some semo-empirical evaporation models

Norris [28] investigated the problem of evaporation from extensive surfaces of water. His analysis was based on a three-layer model which was also used by Montgomery [29]. On physical grounds Norris differed from Montgomery concerning the distribution of water vapor in the outer turbulent layer above rough surfaces. For evaporation from a rough surface, Norris presented the relation

$$E = \rho k u_{*_R} \Gamma_b (q_s - q_b) \tag{13}$$

in which

$$\Gamma_b = \left(\ln \frac{b}{\alpha z_0}\right)^{-1}$$

(in the simplified form) with u_{*_k} and u_{*_R} being the friction velocities in the intermediate and turbulent layers of the three-layer model over a hydrodynamically rough surface and $\ln \alpha = 1.76\, u_{*_k}/u_{*_R}$. From many wind profile data, Norris reported an approximate value of 0·88 for $\ln \alpha$.

Sverdrup [30] used $K_z = ku_*(z + z_0)$ in the relation

$$E = -\rho K_z \frac{\partial q}{\partial z} \tag{14}$$

to obtain (on integration)

$$E = \rho k u_* \left(\ln \frac{b + z_0}{z_0}\right)^{-1} (q_s - q_b). \tag{15}$$

In connection with estimating evaporation losses from lakes, reservoirs, or any other water surfaces of finite extent, let us use the value of mean humidity at 10 m above the water surface as being approximately representative of the ambient humidity. This assumption is compatible with the considerations made in [19]. Determinations of wind profile over the sea [31] indicate that the sea surface is hydrodynamically rough at wind velocities exceeding 6 m/s as measured at a height of 6–12 m above the sea surface. The roughness parameter z_0 of the sea surface was reported to be about 0·6 cm, regardless of the wind velocity. On the other hand, for hydrodynamically rough lake surface, z_0 was found to vary from 0·55 to 1·55 cm for the wind velocity ranging from 1 m/s to 15 m/s measured at 8 m levels from the water surface [19]. An average value of z_0 equal to 0·8 cm was chosen for comparing Norris' [28] and Sverdrup's [30] models with equation (7).

Using the above assumptions, the values of $Ez_0/\rho D(q_s - q_{amb})$ were computed for various values of $u_* z_0/\nu$ from Norris' [28] and Sverdrup's [30] models. The lines representing these models are shown in Fig. 12, along with the results of this study. Agreement is within 10–15 per cent for the range of $u_* z_0/\nu$ considered.

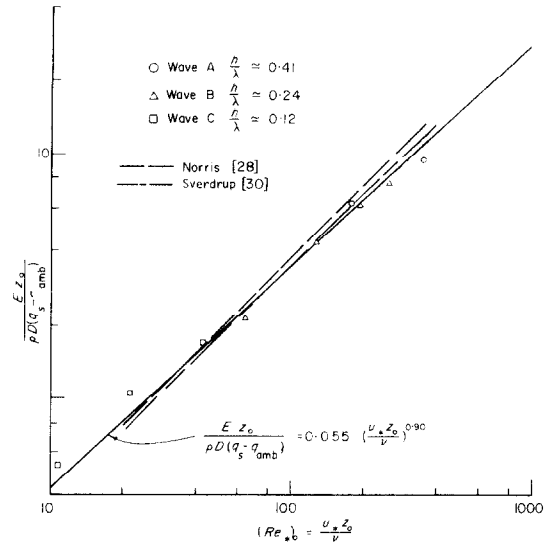

FIG. 12. Comparison with Norris' [28] and Sverdrup's [30] results.

It turns out that the results computed from Norris' [28] and Sverdrup's [30] models are not very sensitive to the chosen level for measuring ambient humidity. For example, a change of this level from 10 to 20 m makes a difference of only 5–8 per cent in the value of $E/q_s - q_{amb}$.

CONCLUDING REMARKS

For uniformly saturated surfaces, the mass transfer parameter $(Sh)_0$, for a wide variety of geometrical characteristics, depends primarily upon the surface Reynolds number $(Re_*)_0$ and the Schmidt number Sc. This implies that the roughness of the surface can influence mass transfer (evaporation, sublimation etc.) rates only insofar as the aerodynamic parameters u_* and z_0 are influenced.

The importance of this result is embodied in the fact that by knowing the wind speed profile above an uniformly saturated surface, one can predict the mass transfer rates with reasonable accuracy for different ambient conditions, provided the surface and ambient concentrations are known.

Acknowledgements—Financial support for research was provided by the U.S. Department of Interior, Office of Water Resources Research, as authorized under the Water Resources Research Act of 1964, Public Law 88-379 and by the Colorado State University Experiment Station under Project 120. The authors wish to thank Drs. M. M. Julliand and F. H. Chaudhry for their assistance at various stages of this work.

REFERENCES

1. W. Nunner, Heat transfer and pressure drop in rough tubes, *VDI ForschHft* Series B, 22, 5–39 (1956).
2. J. W. Smith and N. Epstein, Effect of wall roughness on convective heat transfer in commercial pipes, *A.I.Ch.E.Jl* **3**, 242–248 (1957).
3. D. F. Dipprey and R. H. Sabersky, Heat and momentum transfer in smooth and rough tubes at various Prandtl numbers, *Int. J. Heat Mass Transfer* **6**, 329–353 (1963).
4. N. Pohl, Einfluss der Wandrauhig—keit auf den warmeubergang an Wasser, *Forsch. Ing. Wes.* **4**(5), 230–237 (1933).
5. V. Kolar, Heat and mass transfer in a turbulent medium, *Colln Trav. Chim. Tchécosl.* **26**, 335–345 (1961).
6. V. Kolar, Heat transfer in turbulent flow of fluids through smooth and rough tubes, *Int. J. Heat Mass Transfer* **8**, 639–653 (1965).
7. V. G. Levich, *Physicochemical Hydrodynamics*, Prentice-Hall, Englewood Cliffs, N.J. (1962).
8. D. A. Dawson and O. Trass, Mass transfer at rough surfaces, *Int. J. Heat Mass Transfer* **15**, 1317–1336 (1972).
9. O. G. Sutton, Wind structure and evaporation in a turbulent atmosphere, *Proc. R. Soc.* **146A**, 701–722 (1934).
10. K. L. Calder, Eddy diffusion and evaporation in flow over aerodynamically smooth and rough surfaces, *Q. J. Mech. Appl. Math.* **2**, 153–175 (1949).
11. N. E. Rider, J. R. Phillip and E. F. Bradley, The horizontal transport of heat and moisture—a micrometeorological study, *Q. J. R. Met. Soc.* **89**, 507–531 (1963).
12. S. B. Verma, Mass transfer from rough surfaces, Ph.D. Dissertation, Colorado State University, Fort Collins, Colorado (1971).
13. G. Hsi and J. H. Nath, Wind drag within a simulated forest canopy field, Colorado State University Report No. CER68-69 GH-JHN6 (1968).
14. J. C. Rotta, Turbulent-boundary layer in incompressible flow, *Progress in Aeronautical Sciences*, Vol. 2, edited by A. Ferri, D. Kuchemann and L. H. G. Sterne, p. 120. Pergamon Press, Oxford (1962).
15. A. E. Perry, W. H. Schofield and P. N. Joubert, Rough wall turbulent boundary layers, *J. Fluid Mech.* **37**(2), 383–413 (1969).
16. A. C. Chamberlain, Transport of gases to and from surfaces with bluff and wavelike roughness elements, *Q. J. R. Met. Soc.* **94**, 318–332 (1968).
17. P. R. Owen and W. R. Thomson, Heat transfer from rough surfaces, *J. Fluid Mech.* **15**(3), 321–334 (1963).
18. E. R. G. Eckert and R. M. Drake, Jr., *Heat and Mass Transfer*, McGraw-Hill, New York (1959).
19. J. J. Marciano and G. Earl Harbeck, Jr., Mass-transfer studies, water loss investigations: Vol. 1—Lake Hefner Studies Technical Report, Geological Survey Circular 229, U.S. Department of Interior (1952).
20. B. K. Mahato and L. W. Shemilt, Effect of surface roughness on mass transfer, *Chem. Engng Sci.* **23**, 183–185 (1968).
21. J. Lai, Evaporation from small wind waves, Ph.D. Dissertation, Colorado State University, Fort Collins, Colorado (1969).
22. J. E. Cermak and P. N. Lin, Vapor transfer by forced convection from a smooth, plane boundary, Report No. 55JEC1, Colorado State University, Fort Collins, Colorado (1955).

23. J. E. Cermak and H. J. Koloseus, Lake Hefner model studies on wind structure and evaporation, Report No. 54JEC20, Department of Civil Engineering, Colorado State University, Fort Collins, Colorado (1953).
24. B. M. Smolsky and G. T. Sergeyev, Heat and mass transfer with liquid evaporation, *Int. J. Heat Mass Transfer* **5**, 1011–1021 (1962).
25. E. R. Gilliland and T. K. Sherwood, Diffusion of vapors into air streams, *Ind. Engng Chem.* **26**, 516–523 (1934).
26. T. H. Chilton and A. P. Colburn, Mass transfer (absorption) coefficients—prediction from data on heat transfer and fluid friction, *Ind. Engng Chem.* **26**, 1183–1187 (1934).
27. W. G. Reynolds, W. M. Kays and S. J. Kline, Heat transfer in the turbulent incompressible boundary layer, II—the step temperature distribution, N.A.S.A. Memo 12-2-58W (1958).
28. R. Norris, Evaporation from extensive surfaces of water roughened by waves, *Q. J. R. Met. Soc.* **74**, 1–12 (1948).
29. R. B. Montgomery, Observations of vertical humidity distribution above the ocean surface and their relation to evaporation, Papers in Physical Oceanography and Meteorology, Massachusetts Institute of Technology and Woods Hole Oceanographic Institution, Cambridge and Woods Hole, Massachusetts 7, No. 4, 30 pp. (1940).
30. H. V. Sverdrup, The humidity gradient over the sea surface, *J. Met.* **3**, 1–8 (1946).
31. C. G. Rossby, On the momentum transfer at the sea surface, *Papers in Physical Oceanography and Meteorology* Vol. 4, No. 3, pp. 3–20 (1936).

TRANSFERT DE MASSE A PARTIR DE SURFACE AERODYNAMIQUEMENT RUGUEUSE

Résumé—On a déterminé des flux de transfert de masse en mesurant directement le volume d'eau évaporée à partir de surfaces ondulées (sinusoïdales) saturées, dans une soufflerie micrométéorologique. Des mesures simultanées de distributions de vitesse moyenne, d'humidité et de température ont été pratiquées sur ces ondulations saturées. Dans les conditions de couche limite en équilibre, le coefficient de transfert moyen de masse est une simple fonction puissance du nombre de Reynolds superficiel, $u_* z_0/\nu$. A partir de cette remarque, les points expérimentaux de transfert de masse pour cette étude sont en bon accord avec les résultats publiés sur le transfert de masse pour d'autres types de surfaces (par exemple: ondes d'eau, plaque plane, et surfaces rendues rugueuses avec des pyramides et des excroissances profilées).

STOFFÜBERGANG VON AERODYNAMISCH RAUHEN OBERFLÄCHEN

Zusammenfassung—Der Stoffübergang wird ermittelt durch direkte Messung des jeweiligen Wasservolumens, das von gesättigten welligen (Sinusform) Oberflächen in einem mikrometeorologischen Windkanal verdunstet. Gleichzeitig wurden Messungen der mittleren Geschwindigkeits-, Feuchtigkeits- und Temperatur-Verteilungen über diesen gesättigten Wellenflächen gemacht. Unter Gleichgewichts-Grenzschicht-Bedingungen wurde die mittlere Stoffübergangszahl als einfache Potenzfunktion der Oberflächen-Reynolds-Zahl ($U_* . z_{0/\nu}$) ermittelt. Die ermittelten Stoffübergangsdaten konnten durch dieses Ergebnis recht gut in Übereinstimmung gebracht werden mit veröffentlichen Daten von verschiedenen anderen Oberflächentypen, z.B. Wasserwellen, ebene Platte und Oberflächen, die durch Pyramiden und Buckel aufgerauht sind.

ПЕРЕНОС МАССЫ ОТ АЭРОДИНАМИЧЕСКИ ШЕРОХОВАТЫХ ПОВЕРХНОСТЕЙ

Аннотация — Определялась интенсивность массопереноса непосредственным измерением действительного количества влаги, испаряемой из пропитанных водой волнообразных (синусоидальных) поверхностей в микрометеорологическом воздушном канале. Одновременно измерялись средняя скорость и распределение температуры и влажности над этой волновой поверхностью. Найдено, что осредненный коэффициент массообмена является простой степенной функцией числа Рейнольдса на поверхности, $u_* z_0/\nu$, в условиях равновесного пограничного слоя. Данные по массообмену, полученные в настоящем исследовании, хорошо согласуются с опубликованными данными по массообмену для различных типов поверхностей, например, волн на воде, плоской пластины, поверхностей с шероховатостями в виде пирамид и пологих выступов.